

# INVESTIGATION ON DAM FOUNDATION GROUTING PROCESS

H. SATOH<sup>1</sup>, Y. YAMAGUCHI<sup>1</sup> and T. ABE<sup>2</sup>

<sup>1</sup>Public Works Research Institute, Tsukuba, Japan  
(e-mail of corresponding author: h-sato@pwri.go.jp)

<sup>2</sup>NITTOC Construction CO., LTD., Tokyo, Japan

In dam rock foundations, grouting is performed to improve water-tightness and reinforce weak parts. It is difficult to accurately estimate the improvements brought about by grouting, because the grouting is applied in the rock mass where it is not visible. Recently, research on optimum grout mixtures has advanced and a system that can automatically change the grout mix proportion has been developed. It is possible to change the grouting specifications in order to shorten the injection duration time, if the injection process can be predicted from early grout injection process data. In this paper, we propose a mathematical model, which expresses the injection process of the grouting. Then, we predict the injection duration time and quantity, etc., from early injection process data of the consolidation grouting of an existing dam, using the proposed model and examine the validity of the model.

*Keywords:* Dam Foundation; Grouting; Grout Mix Proportion; Mathematical Model.

## 1. Introduction

In dam rock foundations, grouting is performed to improve the water-tightness and reinforce weak parts (JICE, 2003). It is difficult to accurately estimate the improvements brought about by grouting, because the grouting is injected into the rock mass, where it is invisible.

The Guidelines on Dam Foundation Grouting were revised in 2003 (JICE, 2003), and call for a more systematic approach to grouting with greater attention to foundation conditions. In some foreign countries, the GIN method (Grouting Intensity Number method) (Lombardi, 1996) is used as an injection method to determine optimal grout mix proportions. In Japan, research on optimum grout mix proportions has been conducted and some methods have been proposed, such as the High Thickness-Low Pressure Grouting Method (Mutoh *et al.*, 1999), which injects grout with a relatively dense mix proportion at relatively low pressure. The injection system, which can change the grout mix proportion arbitrarily (Kanden Kogyo, Co., Ltd., 2002, Itoh *et al.*, 2004) has also been developed. It seems possible to change the grouting specifications to shorten the injection duration time, provided the injection process can be predicted from early injection process data of the grouting.

In this study, we propose a mathematical model, which can express the injection process of grouting. Then, we predict the grouting injection duration time and quantity, etc., from early injection process data of the consolidation grouting of an existing dam, using the proposed model and examine the validity of the model.

## 2. Numerical model and formula

In order to predict the grouting process based on early injection grouting data, it is necessary to develop a numerical model capable of describing the grouting injection process.

Mutoh *et al.* (1999) have developed a grouting injection model with particular emphasis on change in the cross-sectional area of the joints. Predictions generated by the model were compared with the results of injection tests using an experimental apparatus built with transparent pipes.

We propose the following, simplified model for the grouting injection process, designed to

enable overall evaluation of grouting injection into complex ground foundations. The model assumes a cube law between crack width and grouting flow rate.

$$\frac{Q_t}{P_t} = \alpha(D_0 - \beta t)^3 \frac{1}{\mu} \quad (1)$$

where

- $t$  : duration time from the beginning of injection (min)
- $Q_t$  : grouting injection rate at  $t$  (l/min/m)
- $P_t$  : effective grouting pressure at  $t$  (MPa)
- $D_0$  : average crack width at  $t=0$  (m)
- $\mu$  : viscosity of cement milk / viscosity of water
- $\alpha$  : a constant based on the number of cracks (l/min/m<sup>4</sup>/0.98MPa)
- $\beta$  : a constant based on the crack filling speed (m/min)

Eq. (1) describes the process by which: (1) the crack width becomes smaller over time because cracks are filled with injected grout and; (2) the injection quantity decreases according to the decreased crack width. The term  $(D_0 - \beta t)$  in Eq. (1) represents the crack width narrowing over time as the crack is filled with cement milk. The grout flow is assumed to be laminar in Eq. (1). The  $\alpha$  is related to the number of cracks in the injection hole; the higher the value of  $\alpha$ , the greater the number of cracks in the injection hole. The  $\beta$  is related to the grout filling speed, and is governed by factors such as the cement milk mix proportion and the injection flow rate. A higher  $\beta$  value means that the cracks are filled more quickly.

If the critical pressure does not occur, then at  $t=0$ ,  $0.98Q_t\mu/P_t$  is equivalent to the Lugeon value. Thus, the Lugeon value before injection can be expressed as follows:

$$Lu_0 = 0.98\alpha D_0^3 \quad (2)$$

From Eq. (2), by using the initial Lugeon value for the injection hole, we can determine either  $\alpha$  or  $D_0$ . Substituting  $\alpha$  from Eq. (2) into Eq. (1) and reconfiguring the expression produces Eq. (3) below. Then, by determining  $\beta/D_0$ , based on early observed injection data, it should be possible to predict the subsequent injection process.

$$\frac{Q_t}{P_t} = \frac{Lu_0}{0.98} \left(1 - \frac{\beta}{D_0} t\right)^3 \frac{1}{\mu} \quad (3)$$

### 3. Details of an existing dam investigated

This study involves an analysis based on minute-by-minute time-series data on flow rate, injection pressure and mix proportion during the injection process. Table 1 lists the main statistics of an existing concrete gravity dam used in the analysis. The data was taken at 5BL in the left bank, which had a relatively high initial permeability. Data under 2 Lugeon is omitted from the analysis, because injection into such low permeability area tended to be completed quickly. Besides, data obtained from substantially different injection conditions are also omitted. As a result, 73 data in total are used in the analysis. Table 2 shows the details of injection specifications.

Table 1. Specification of dam studied

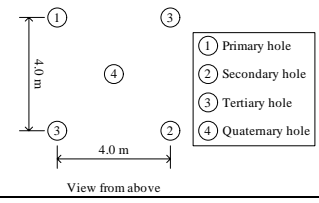
Type of dam	Concrete gravity dam
Height	114.0 m
Crest length	331.3 m
Volume	750,000 m <sup>3</sup>
Geology	Mesozoic Era, Cretaceous Period Granite

#### 4. Conditions for data analysis

The following conditions are considered investigating the time history data of actual grout injection, in order to examine how accurately the model in Eq. (1) describes the grouting injection process.

- (1) The initial Lugeon value  $Lu_0$  is calculated based on pressure, grout flow and mix proportion (viscosity) data before grout flow or injection pressure reaches the specified flow rate value (or pressure).
- (2) Viscosity of cement milk is affected by changes in temperature, and also by the shear speed in cracks (Tani *et al.*, 1999). However, for the sake of simplicity, the model assumes that viscosity is affected only by the mix proportion, and not by temperature nor shear speed.
- (3) The electronic data shows sudden changes in the injected mix proportion at certain stages in the grouting process. During actual grouting, however, some of the new milk is introduced prior to the change in mix proportion, in order to make the change gentler. The model simulates this situation by assuming a simple linear transformation of the mix proportion as shown in Fig. 1.

Table 2. Injection specification

Improvement target value	5 Lugeon																															
Construction time	After dam body concrete placement over 3 m																															
Layout of grout holes																																
Depth of grout holes	5 m																															
Water pressure test	Pressure steps (MPa) : 0.05 0.1 0.15 0.2 0.25 0.3																															
Grouting	Material : Portland blast-furnace slag cement Max injection pressure : 0.3 MPa Max grout flow rate : 4 L/min/m																															
	Change of grout mix :																															
	<table border="1"> <thead> <tr> <th>Lugeon</th> <th>Lu &lt; 10</th> <th>10 &lt; Lu &lt; 20</th> <th>20 &lt; Lu</th> </tr> </thead> <tbody> <tr> <td>10</td> <td>400 l</td> <td>-</td> <td>-</td> </tr> <tr> <td>6</td> <td>400 l</td> <td>400 l</td> <td>-</td> </tr> <tr> <td>4</td> <td>400 l</td> <td>400 l</td> <td>400 l</td> </tr> <tr> <td>3</td> <td>400 l</td> <td>400 l</td> <td>400 l</td> </tr> <tr> <td>2</td> <td>600 l</td> <td>600 l</td> <td>600 l</td> </tr> <tr> <td>1</td> <td>800 l</td> <td>1200 l</td> <td>1600 l</td> </tr> <tr> <td>Total</td> <td>3000 l</td> <td>3000 l</td> <td>3000 l</td> </tr> </tbody> </table>	Lugeon	Lu < 10	10 < Lu < 20	20 < Lu	10	400 l	-	-	6	400 l	400 l	-	4	400 l	400 l	400 l	3	400 l	400 l	400 l	2	600 l	600 l	600 l	1	800 l	1200 l	1600 l	Total	3000 l	3000 l
Lugeon	Lu < 10	10 < Lu < 20	20 < Lu																													
10	400 l	-	-																													
6	400 l	400 l	-																													
4	400 l	400 l	400 l																													
3	400 l	400 l	400 l																													
2	600 l	600 l	600 l																													
1	800 l	1200 l	1600 l																													
Total	3000 l	3000 l	3000 l																													

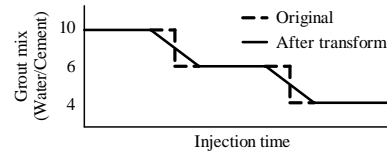


Fig. 1. Change of grout mix

#### 5. Results

##### 5.1. Classification of injection patterns

The following comparative analysis is used to assess the ability of the proposed model to describe the grouting injection process.

- (1) The initial Lugeon value  $Lu_0$  is calculated from the flow rate, pressure and mix proportion (viscosity) at the commencement of injection.
- (2) Eq. (3) is used to determine the value of  $\beta/D_0$  by the least-squares method using the observed values for flow rate, pressure and mix proportion (viscosity) and the initial Lugeon value  $Lu_0$ .
- (3) The  $\beta/D_0$  and  $Lu_0$  values are obtained in (1) and (2). These values and the observed injection mix proportion (viscosity) data are substituted for Eq. (3), in order to find  $Q_i/P_i$  at any point in time.
- (4) The observed injection chart is compared with the calculated injection chart in (3).

The above analysis yields three distinct patterns based on their shapes. Table 3 shows the results

of the classification. More than half of the data corresponds to Pattern I, where the calculated values are very consistent with observed values. Pattern II is where the observed injection data drops sharply in the early injection duration time, while Pattern III shows a milder decreasing curve in the early injection duration time. Examples of the three patterns are illustrated in Figs. 2 to 4.

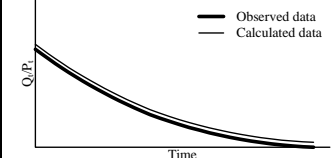
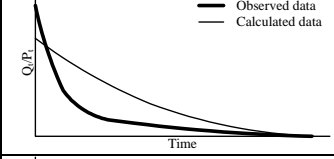
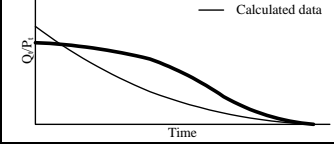
### 5.2. Prediction of injection duration time and quantity

Injection duration time and quantity are predicted as described below, using the model proposed in this paper, based on early injection data obtained at 11, 21 and 31 minutes. To simplify the prediction process, the value of  $\beta/D_0$  is calculated by one data derived only at one time.  $Lu_0$  value is obtained from the early injection data as described in 5.1. (1).

- (1) For each injection hole, the  $Lu_0$  value from early injection data, and observed values  $Q_i$ ,  $P_i$  and  $\mu$  measured at 11, 21 and 31 minutes are substituted for Eq. (3) to find  $\beta/D_0$ .
- (2) The  $\beta/D_0$  values obtained in (1), observed values of  $P_i$  and  $\mu$ , and  $Lu_0$  value are substituted for Eq. (3), in order to estimate values for  $Q_i$  at any point in time. This expression is then used to plot the calculated chart for  $Q_i$ .
- (3) An extra 30 minutes is added to the predicted injection duration time when the injection rate reaches 0.2 l/min/m. The injected quantity is defined as the sum total of the flow rates, calculated at one-minute intervals, from the beginning of the injection process to the end.

Figs. 5 and 6 show the comparisons of the injection duration times and injection quantities, between observed values and calculated values at 11, 21 and 31 minutes. In Figs. 5 and 6, plots are classified

Table 3. Pattern types

Pattern	Grouting injection process	Number of data
I		37
II		31
III		5
All 73 data		

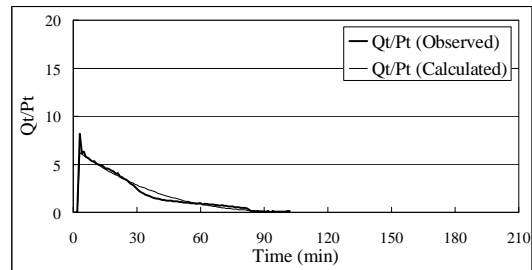


Fig. 2 Example of pattern I (C05-A43030)

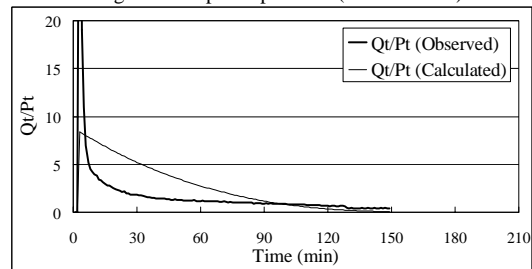


Fig. 3 Example of pattern II (C05-A53340)

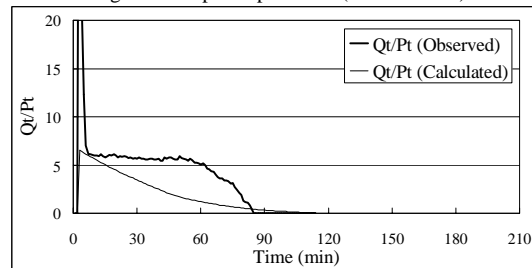


Fig. 4 Example of pattern III (C05-A32940)

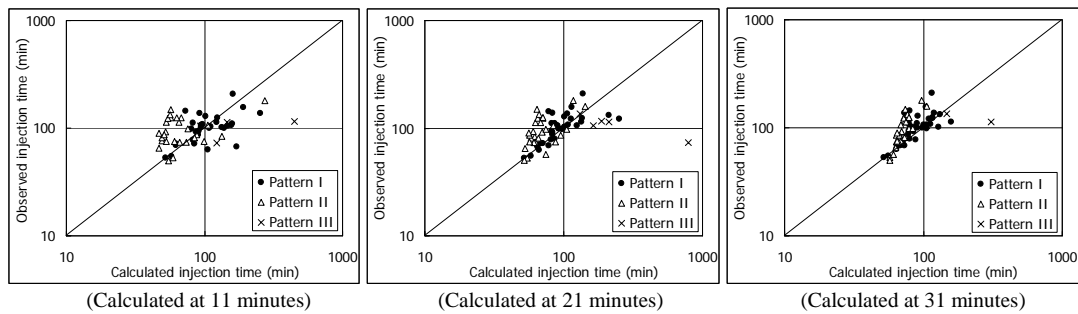


Fig. 5 Injection time of observed data and calculated data

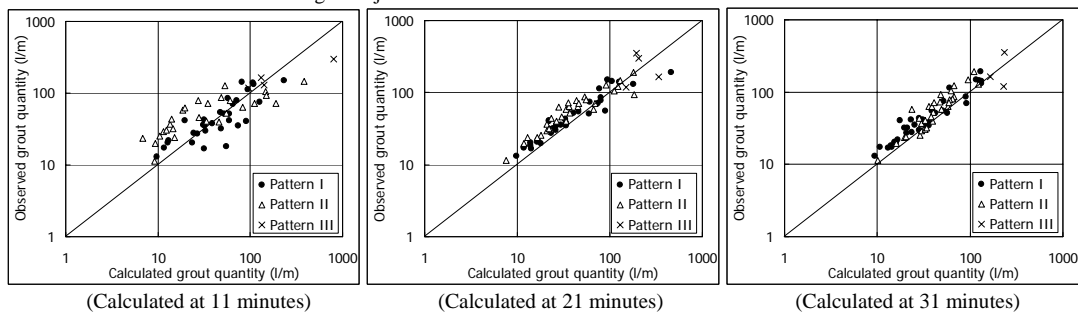


Fig. 6 Grout quantity of observed data and calculated data

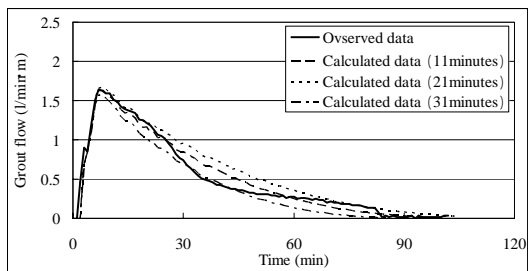


Fig. 7 Comparison of observed data and calculated data (C05-A43030)

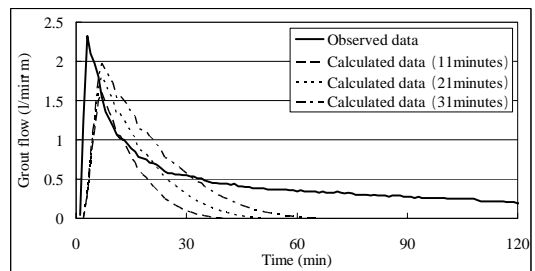


Fig. 8 Comparison of observed data and calculated data (C05-A53340)

according to the three patterns described in 5.1. Figs. 7 and 8 show examples of observed charts and calculated charts from data at 11, 21 and 31 minutes. The curves in Fig. 7 are fairly consistent, but in Fig. 8 the discrepancy in grout flow increases with time.

Overall, there is a considerable difference in injection duration time between the observed and calculated values. The differences between the observed results and the calculated results from data at 11 minutes tend to be greater than those at 21 and 31 minutes. From Fig. 5, Pattern I data are generally clustered together in a one-to-one linear relationship and are more conducive to accurate calculation. Pattern II has slightly more differences than Pattern I and the calculated injection duration times tend to be shorter than the observed times. Pattern III data show the biggest differences and the calculation accuracy is not good.

The calculated injection quantities shows greater variance at 11 minutes in all three patterns compared to the data for 21 and 31 minutes, which locate in a one-to-one linear distribution, indicating accurate prediction. The greater variance at 11 minutes can be attributed to the influence of unsteady factors in the early injection duration time, which results in increasing flow rates. Then, such large flow rates require at least ten minutes to stabilize. These unsteady factors seem to largely disappear at around 21 minutes, and the prediction data improve. Even the data

calculated at 21 and 31 minutes is generally located on a one-to-one linear relationship; the observed values for flow rate generally tend to be slightly higher than calculated values. This is also attributed to the sudden increase in flow rate due to unsteady factors that tend to boost the observed injection quantity values slightly.

Judging from these results, it can be concluded that the proposed model provides a valid method for predicting the flow rate from data obtained after 20 minutes, notwithstanding a certain degree of difficulty in predicting of injection duration time.

## 6. Detailed Analysis of Patterns II and III

We have shown that the model proposed in this study produces a generally reliable description of the grouting process with respect to Pattern I injection charts, providing accurate prediction of the injection quantity. Patterns II and III, however, despite providing reasonable accuracy in respect of injection quantity, cannot predict the whole injection process with sufficient reliability. We investigate the reasons why the model is unable to provide sufficient accuracy for Patterns II and III.

### 6.1. Pattern II

Experience suggests that the injection chart seen in Pattern II is typically found with rock foundation where the permeability is relatively high but the injection quantity is small, such as rock foundation containing weathered granite because the cement milk is unable to penetrate as readily as water.

So far, we have investigated how accurately the model can describe the injection process, based on a single set of parameters ( $0.98\alpha D_0^3 (= Lu_0)$  and  $\beta/D_0$ ). In this section, we will try to fit the model using two sets of parameters: the first,  $0.98\alpha_1 D_{01}^3$  and  $\beta_1/D_{01}$ , for the early injection duration time at  $t=t_1$  when the flow rate decreases rapidly; and the second,  $0.98\alpha_2 D_{02}^3$  and  $\beta_2/D_{02}$ , for the time later than  $t_1$  when the flow rate stabilizes and decreases gradually. Fig. 9 shows an example of fitting the result to the Pattern II injection chart, using two sets of parameters, with the injection process divided into two sections delineated at the 13-minute mark. For the calculated injection chart with the second pair of parameters,  $0.98\alpha_2 D_{02}^3$  and  $\beta_2/D_{02}$ , the  $0.98\alpha_2 D_{02}^3$  value equivalent to  $Lu_0$  is calculated based on the first

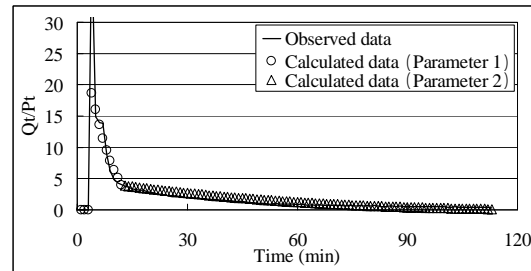


Fig. 9 Example of the two sets of parameters fit (C05-A42630)

Table 4. Values of parameters (C05-A42630)

Parameter	$\alpha$ is invariable ( $\alpha_1 = \alpha_2$ )	$\beta$ is invariable ( $\beta_1 = \beta_2$ )	$D_0$ is invariable ( $D_{01} = D_{02}$ )
$\alpha_1$	$\alpha_1$	$3.6 \times 10^{-3} / \beta_1^3$	$49.0 / D_{01}^3$
$\beta_1$	$0.153 \alpha_1^{1/3}$	$\beta_1$	$0.0418 D_{01}$
$D_{01}$	$3.66 \alpha_1^{1/3}$	$24.0 \beta_1$	$D_{01}$
$\alpha_2$	$\alpha_1$	$1.7 \times 10^{-6} / \beta_1^3$	$7.6 / D_{01}^3$
$\beta_2$	$0.012 \alpha_1^{1/3}$	$\beta_1$	$0.00614 D_{01}$
$D_{02}$	$1.96 \alpha_1^{1/3}$	$162.9 \beta_1$	$D_{01}$

Table 5. Relationship of  $\alpha$ ,  $\beta$  and  $D_0$  (Pattern II)

$\alpha$ is invariable	$\beta$ is invariable	$D_0$ is invariable
$\alpha_1 = \alpha_2$	$\alpha_1 > \alpha_2$	$\alpha_1 > \alpha_2$
$\beta_1 > \beta_2$	$\beta_1 = \beta_2$	$\beta_1 > \beta_2$
$D_{01} > D_{02}$	$D_{01} < D_{02}$	$D_{01} = D_{02}$

prediction data from  $0.98\alpha D_0^3 (= Lu_0)$  and  $\beta/D_0$ , instead of using  $Lu_0$ .

To investigate the influences of each parameter in detail, we conducted a parametric study: one parameter was set to be constant while other parameters were changed as shown in Table 4. Table 4 gives example values for the chart shown in Fig. 9. The results of fitting the data to Pattern II generally exhibit the relationship shown in Table 5. The meaning and significance of each parameter is discussed below.

As for  $\alpha$  and  $\beta$ , the values in the early injection process are larger than those in the later injection process. Because  $\alpha$  is governed by the number of cracks and  $\beta$  by the crack filling speed, and because the thinner cracks are closed up at an early injection time and the flow rate declines with time, so  $\alpha$  and  $\beta$  are thought to decrease with the progress of injection as shown in Table 5.

As for  $D_0$ , the results show such that  $D_{01} > D_{02}$  when  $\alpha_1 = \alpha_2$  and  $D_{01} < D_{02}$  when  $\beta_1 = \beta_2$ . Because  $D_0$  is the parameter for the average crack width within an injection hole,  $D_{01} < D_{02}$  means that the average crack width becomes wider with the progress of injection. This result seems strange, but this is because of the fact that in this study we have used a single parameter for the average crack width,  $D_0$ , to represent crack widths in an injection hole, whereas in actual foundations there will be many cracks of varying widths. Another reason for  $D_{01} < D_{02}$  is that narrower cracks are easily filled during the early injection time, so the calculated average crack width,  $D_0$ , will become larger over time.

## 6.2. Pattern III

Pattern III is often seen in high permeability, high injection quantity foundation rock. Since this study uses data mainly for low injection quantities, the number of data corresponding to Pattern III is small. Three parameters are used to fit the Pattern III injection chart: (1)  $0.98\alpha_1 D_{01}^3$  and  $\beta_1/D_{01}$  for the early injection time with gently decreasing of flow rate, (2)  $0.98\alpha_2 D_{02}^3$  and  $\beta_2/D_{02}$  when the flow rate starts decreasing more quickly, and (3)  $0.98\alpha_3 D_{03}^3$  and  $\beta_3/D_{03}$  when the flow rate decreases gently again. Fig. 10 shows a result, with the process divided into three distinct periods delineated at 23- and 48-minute marks. Similar to Pattern II described in 6.1,  $0.98\alpha_2 D_{02}^3$  and  $0.98\alpha_3 D_{03}^3$  are calculated using initial data for the second and third processes, respectively. Parameters for Pattern III generally show the relationship in Table 6.

Because Pattern III is often seen in high-permeability foundations, the flow in cracks easily becomes turbulent, while the model assumes a laminar and other factors might also influence the injection mechanism. The  $\beta$  value in particular seems to be susceptible to changes in flow rate, mix proportion, pressure and crack width during the injection process.

In general, flow rates in Patterns II and III tend to be influenced by a complex combination of many factors, rather than by

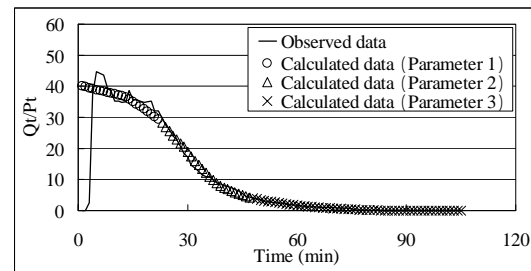


Fig. 10 Example of the two sets of parameters fit (C05-A73740)

Table 6. Relationship of  $\alpha$ ,  $\beta$  and  $D_0$  (Pattern III)

$\alpha$ is invariable	$\beta$ is invariable	$D_0$ is invariable
$\alpha_1 = \alpha_2 = \alpha_3$	$\alpha_1 < \alpha_2 > \alpha_3$	$\alpha_1 < \alpha_2 > \alpha_3$
$\beta_1 < \beta_2 > \beta_3$	$\beta_1 = \beta_2 = \beta_3$	$\beta_1 < \beta_2 > \beta_3$
$D_{01} < D_{02} > D_{03}$	$D_{01} > D_{02} < D_{03}$	$D_{01} = D_{02} = D_{03}$

any single factor.

## 7. Conclusions

A numerical model was proposed in this paper to predict injection duration time and quantities from observed data derived from early injection duration time. We used data obtained from consolidation grouting of an existing dam. The model is able to predict injection quantities fairly accurately, although prediction of injection duration time is less successful. For roughly half the data, the grouting injection process can be described satisfactorily using a single set of  $\alpha$  and  $D_0$  values in Pattern I, but for injection charts corresponding to Patterns II and III, one set of parameters is not sufficient, and it is necessary to use two or even three sets of  $\alpha$  and  $D_0$  values, calculated at different time.

The study described in this paper used data from a specific area of a single dam. Further study is needed to examine the validity of this study, using data in other types of foundations with different geology and permeability, in order to provide a more accurate model. This model can also be used to identify the major parameters affecting injection, in order to develop more rational and practical approaches to dam foundation grouting.

## References

- Japan Institute of Construction Engineering (2003). "Guidelines on Dam Foundation Grouting" (In Japanese).
- G. Lombardi (1996). "Selecting the grouting intensity", *Hydropower & Dams*, Issue 4 .
- Hikaru Mutoh et al. (1999). "Suggestion of High Thickness-Low Pressure Grouting Method (HTLP Method)", *J. JSDE*, Vol. 9, No. 3, 201–214 (In Japanese).
- Kanden Kogyo Co., Ltd. (2002). "The KK Automated Grouting System", *Dam Technology*, No. 185, 58–61 (In Japanese).
- Setsuo Ito et al. (2004). "Development and Application of a Variable Mix Injection System", *Proc. The 2004 Civil Engineering and Construction Technology Symposium*, Japan Society of Civil Engineers, 133–138 (In Japanese).
- Hikaru Mutoh et al. (1999). "Experimental Study on Grouting Mechanism in Jointed Rock Masses using Transparent Tubes", *J. JSDE*, Vol. 9, No. 1, 29–38 (In Japanese).
- Satoshi Tani and Yoshihisa Uchida (1999). "Relationship between Density and Flow Properties of Cement Suspension", *J. JSDE*, Vol. 9, No. 3, 175–186 (In Japanese).